Plant, Cell & Environment

Plant, Cell and Environment (2011) **34**, 778–791 doi: 10.1111/j.1365-3040.2011.02281.x

Complexation of Hg with phytochelatins is important for plant Hg tolerance

SANDRA CARRASCO-GIL[1,3]*, ANA ÁLVAREZ-FERNÁNDEZ[4]*, JUAN SOBRINO-PLATA,[1] ROCÍO MILLÁN,[3] RAMÓN O. CARPENA-RUIZ,[2] DANIKA L. LEDUC,[5] JOY C. ANDREWS,[5,6] JAVIER ABADÍA[4] & LUÍS E. HERNÁNDEZ[1]

[1]Laboratory of Plant Physiology, Department of Biology, [2]Department of Agricultural Chemistry, Universidad Autónoma de Madrid, 28049 Madrid, [3]Centro de Investigaciones Energéticas, Medioambientales y Tecnológicas, Avd. Complutense, 22, 28040 Madrid, [4]Department of Plant Nutrition, Estación Experimental de Aula Dei-CSIC, P.O. Box 13034, 50080 Zaragoza, Spain, [5]Department of Chemistry and Biochemistry, California State University, East Bay 25800 Carlos Bee Boulevard, Hayward and [6]Stanford Synchrotron Radiation Lightsource, 2575 Sand Hill Road, SLAC MS 69 Menlo Park, CA, USA

ABSTRACT

Three-week-old alfalfa (*Medicago sativa*), barley (*Hordeum vulgare*) and maize (*Zea mays*) were exposed for 7 d to 30 μM of mercury ($HgCl_2$) to characterize the Hg speciation in root, with no symptoms of being poisoned. The largest pool (99%) was associated with the particulate fraction, whereas the soluble fraction (SF) accounted for a minor proportion (<1%). Liquid chromatography coupled with electro-spray/time of flight mass spectrometry showed that Hg was bound to an array of phytochelatins (PCs) in root SF, which was particularly varied in alfalfa (eight ligands and five stoichiometries), a species that also accumulated homophytochelatins. Spatial localization of Hg in alfalfa roots by microprobe synchrotron X-ray fluorescence spectroscopy showed that most of the Hg co-localized with sulphur in the vascular cylinder. Extended X-ray Absorption Fine Structure (EXAFS) fingerprint fitting revealed that Hg was bound *in vivo* to organic-S compounds, i.e. biomolecules containing cysteine. Albeit a minor proportion of total Hg, Hg–PCs complexes in the SF might be important for tolerance to Hg, as was found with *Arabidopsis thaliana* mutants *cad2-1* (with low glutathione content) and *cad1-3* (unable to synthesize PCs) in comparison with wild type plants. Interestingly, high-performance liquid chromatography-electrospray ionization-time of flight analysis showed that none of these mutants accumulated Hg–biothiol complexes.

Key-words: biothiols; EXAFS; mass spectrometry; mercury; phytochelatins; soluble fraction; X-ray absorption spectroscopy.

Abbreviations: DEAE, diethylaminoethyl; DTT, dithiothreitol; GSH, glutathione; hGSH, homoglutahione; hPCs, homophytochelatins; MF, microsomal fraction; PCs, phytochelatins; PF, particulate fraction; SF, soluble fraction.

Correspondence: L. E. Hernández. Fax: +34 914978344; e-mail: luise.hernandez@uam.es

*S.C.G and A.A.F. contributed equally to this work.

INTRODUCTION

Mercury (Hg) accumulation is considered a global environmental threat, and its trade is restricted due to its bioaccumulation and biomagnification in diverse ecosystems (Leonard *et al*. 1998). Mercury has no nutritional role, and exposure of biological systems to relatively low Hg concentrations results in serious toxicity (Nriagu 1990). Although little is known about the precise mechanism of toxicity exerted by Hg in plants, cellular integrity and biological activity might be compromised due to its strong affinity for sulfhydryl residues of proteins and other biomolecules (Van Assche & Clijsters 1990; Hall 2002). Mercury has also been found to be a potent inducer of oxidative stress (Cho & Park 2000; Rellán-Álvarez *et al*. 2006a), and an oxidative burst appeared in alfalfa root epidermal cells after a brief exposure to 30 μM Hg (Ortega-Villasante *et al*. 2007), in spite of its limited redox activity (Schützendübel & Polle 2002).

Mercury accumulates preferentially in roots (4- to 10-fold the concentration found in shoots) of several plant species such as *Pisum sativum* (Beauford, Barber & Barringer 1977), *Brassica napus* (Iglesia-Turiño *et al*. 2006), *Zea mays* (Rellán-Álvarez *et al*. 2006a) and *B. chinensis* (Chen, Yang & Wang 2009). Therefore, most of the toxic effects of Hg are observed in roots. A large proportion of Hg was found associated with cell wall materials in *P. sativum* and *Mentha spicata* (Beauford *et al*. 1977), *Nicotiana tabacum* (Suszcynsky & Shann 1995) and *Halimione portulacoides* (Válega *et al*. 2009). Although the mobility of Hg within the plant may be limited by root cell walls, the distribution in root cells or tissues is not presently clear. This objective can be achieved using techniques such as microprobe synchrotron X-ray fluorescence spectrometry (μ-SXRF), which is capable of providing spatially resolved metal data (Punshon, Guerinot & Lanzirotti 2009).

Once heavy metals enter the cell, additional defence mechanisms involve the synthesis of organic ligands that could form metal complexes with reduced biological activity. Among these compounds, phytochelatins (PCs) are known to bind Cd and other toxic elements by means of

sulfhydryl residues (Cobbett & Goldsbrough 2002). Phytochelatins are synthesized from glutathione (GSH) and homologous biothiols by the enzyme phytochelatin synthase (PCS; Grill *et al*. 1989; Clemens *et al*. 1999; Vatamaniuk *et al*. 1999 and Ha *et al*. 1999). When plants are exposed to heavy metals, PCS condenses the γ-glutamyl-cysteine (GC) moiety of a GSH molecule with the glutamic acid residue of a second GSH, releasing glycine and increasing the length of the PC molecule (Vatamaniuk *et al*. 2004; Clemens 2006).

Significant amounts of free PCs were detected in Hg-treated *Brassica napus* plants with high-performance liquid chromatography coupled to mass spectrometry (HPLC-MS) after removal of Hg with a strong Hg-specific chelator (Iglesia-Turiño *et al*. 2006). Phytochelatins were also found in maize and alfalfa plantlets grown with Hg, but in lower amounts than in Cd-treated plants (Rellán-Álvarez *et al*. 2006a; Sobrino-Plata *et al*. 2009). *In vitro* studies using HPLC-MS also showed that small biothiols such as GSH and cysteine bind Hg (Krupp *et al*. 2008; Chen *et al*. 2009).

X-ray absorption spectroscopy (XAS) is a non-destructive technical approach that can be used for speciating metals in plant tissues (Aldrich *et al*. 2003, Gardea-Torresdey *et al*. 2003; Pickering *et al*. 2003; De la Rosa *et al*. 2004). Understanding metal speciation is essential to clarify detoxification mechanisms in plants (Arruda & Azevedo 2009). Synchrotron-based techniques, widely utilized to study metal chemical properties in a vast array of materials (i.e. composites, semiconductors, etc.), are increasingly being used to characterize metal speciation in biological materials such as plants (Salt, Prince & Pickering 2002). Among different methods of analysis, X-ray absorption near edge spectroscopy (XANES) and extended X-ray absorption fine structure (EXAFS) provide information about a target atom (oxidation state, local geometry, local environment, co-ordination numbers and bond lengths) in close-to-natural-state plant tissues. Both techniques have been recently used to characterize the speciation of Hg in *Spartina foliosa* and *Eichhornia crassipes* (Riddle *et al*. 2002; Rajan *et al*. 2008; Patty *et al*. 2009). However, fingerprint fitting of XANES and EXAFS spectra, the method used in this paper, require standards of metal–ligand complexes putatively occurring in plant tissues (Kim, Brown & Rytuba 2000).

In spite of the evidence pointing towards a role for PCs in Hg complexation in higher plants, only a small number of Hg–PC complexes have been found using HPLC-MS in root extracts of *B. chinensis*, *Oryza sativa* and *Marrubium vulgare* (Chen *et al*. 2009; Krupp *et al*. 2009). In the present study, a combined approach using both *in vivo* analysis by XAS and HPLC coupled to a high-resolution mass analyser (time-of-flight; TOFMS) was used to elucidate the plant components involved in the effective defence mechanisms utilized by three week old alfalfa (*Medicago sativa*), barley (*Hordeum vulgare*) and maize (*Z. mays*) plants exposed for 7 d to 30 μM of mercury (Hg, as $HgCl_2$). This high concentration of Hg was used in a short-term treatment to provide an adequate detection level of Hg with the techniques used in our studies, since the distribution and speciation of metals in non-hyperaccumulator plants is technically more challenging due to the lower concentration of the analyte (Lombi & Susini, 2009). Moreover, a functional analysis with *Arabidopsis thaliana* mutants *cad2-1*, with diminished γ-glutamylcysteine synthetase activity (Cobbett *et al*. 1998), and *cad1-3*, defective in PCS activity (Howden *et al*. 1995), were used to evaluate Hg tolerance and Hg–biothiol complexes formation relative to wild-type Col-0 plants.

MATERIALS AND METHODS

Plant material

Alfalfa (*M. sativa* cv. Aragon), maize (*Z. mays* cv. Dekalb Paolo) and barley (*H. vulgare*) seedlings were germinated and grown in a semi-hydroponic system as described by Sobrino-Plata *et al*. (2009) for alfalfa and as by Rellán-Álvarez *et al*. (2006a) for maize and barley. The plants grew for 12 d in a controlled environment chamber and were then treated with 30 μM Hg (as $HgCl_2$) for 7 d. Once collected, plants were rinsed several times with 10 mM Na_2 EDTA solution to remove superficial Hg, and roots were harvested for tissue fractionation. Another portion of plants were used to determine total Hg concentration in tissues. In some experiments to more easily detect Hg by atomic absorption spectrophotometry in diethylaminoethyl (DEAE)-eluted fractions or by XAS spectroscopy in intact roots (see further discussion), several batches of maize and alfalfa plantlets were grown in a pure hydroponic system with continuous aeration (Ortega-Villasante *et al*. 2005).

Tolerance to Hg assay

Functional experiments of Hg–complexation by PCs were performed with *A. thaliana* mutants with altered biothiol content. Col-0, *cad2-1* and *cad1-3* seeds were grown for 12 d in square Petri dishes in solid Murashige-Skoog nutrient medium (0.6% phyto agar, Duchefa Biochemie B.V., Haarlem, the Netherlands) supplemented with 2% sucrose. Tolerance was assessed by measuring root growth after exposure to 10 μM Hg, supplied in soaked 3MM filter paper (Whatman, Maidstone-Kent, UK) strips (10 × 1 cm) for 5 d in plates that were rotated 180° (roots-up position). Biothiol profile of mutant *A. thaliana* was studied in the leaves of plants (grown in a perlite-peat mixture for three weeks in short-days light regime), which were infiltrated under vacuum with water, 30 μM Cd or 30 μM Hg, and incubated for 48 h.

Tissue fractionation

Root tissue fractions were prepared following the procedure described by Lozano-Rodríguez *et al*. (1997). The homogenate was centrifuged at 10 000 g for 30 min, and the pellet, consisting mainly of cell walls, intact cells and organelles, was labelled the Particulate Fraction (PF). The remaining supernatant was centrifuged again at 100 000 g

for 30 min. The pellet contained membrane fragments and constituted the Microsomal Fraction (MF). The supernatant contained all soluble components of the cell, constituting the so-called Soluble Fraction (SF). All steps were performed at 4 °C, and the fractions were stored at –20 °C for further analysis.

Anion exchange chromatography of root soluble fractions

The maize root SF was analysed by anion exchange chromatography to determine the possible association of Hg to biothiols. An XK26 C-16/40 column (Phamacia Biotech, Uppsala, Sweden) filled with DEAE fast flow Sepharose (Sigma-Aldrich, St. Louis, MO, USA) was equilibrated with 10 mM Tris–HCl washing buffer (pH 8.6) using a peristaltic pump (1.8 mL/min flow; Gilson, Middleton, WI). The column was loaded with 35 mL of SF and washed until a baseline elution was achieved by measuring absorbance at $\lambda = 340$ nm with a UA-5 UV detector (Teledyne ISCO, Lincoln, NE, USA). Elution was achieved using washing buffer supplemented with 0.5 M NaCl. Fractions (2.3 mL) were collected until the baseline was reached and stored at –20 °C for further analysis.

Biothiol analysis

A 300 μL aliquot of each DEAE chromatography fraction was used to determine the total biothiol content. Ice-cold 20% TCA (50 μL) was added to precipitate proteins, and the mixture was then centrifuged at 10 000 g for 15 min at 4 °C. The supernatant (100 μL) was mixed with 400 μL of reducing solution (1 M NaOH, 1 mg mL^{-1} $NaBH_4$) and 200 μL analytical-grade type II water (miliRO, Millipore, Bedford, MA, USA). After acidification with 100 μL 35% HCl, biothiols were detected after the addition of 600 μL of Ellman's reagent (300 μM 5,5′-Dithiobis(2-nitrobenzoic acid) in 0.5 M NaH_2PO_4, pH 7.5) by measuring the absorbance at 412 nm (Shimadzu UV-2401PC spectrometer, Kyoto, Japan). Biothiol concentration was calculated using a GSH standard curve. Biothiol profile of *A. thaliana* plants was analysed by HPLC as described by Ortega-Villasante *et al*. (2005).

Mercury analysis

Solid samples of roots and cell wall fractions were dried at 40 °C to constant weight and ground with mortar and pestle. Dried plant material (100 mg) was acid digested in 2 mL of the digestion mixture (HNO_3:H_2O_2:H_2O, 0.6:0.4:1 v:v) in an autoclave (Presoclave-75 Selecta, Barcelona, Spain) at 120 °C and 1.5 atm for 30 min (Ortega-Villasante *et al*. 2007). Liquid samples (500 μL), including microsomal, soluble and DEAE chromatography fractions, were directly digested as described earlier after the addition of 300 μL HNO_3 and 200 μL H_2O_2. The digests were filtered through a polyvinylidene fluoride filter and diluted in miliRO water to 10 mL. Hg concentration was measured by atomic absorption spectrophotometry, either with an Advanced Mercury Analyser 254 Leco (St. Joseph, Michigan, MI, USA) or with a Atomic Absorption Spectrophotometer Model 4000 equipped with a $NaBH_4$ cold vapour chamber MSH-20 (Perkin Elmer, Wellesley, MA, USA).

Preparation of biothiol and Hg–biothiol complex standard solutions

Biothiol stock standard solutions containing from 2 to 4 mM of GSH (M_m 307.3; Sigma-Aldrich), hGSH (M_m 321.4; Bachem, Bubendorf, Switzerland), γ-(Glu-Cys)$_2$ (GC_2; M_m 482.5; GenScript Corporation, Scotch Plains, NJ, USA), γ-(Glu-Cys)$_2$-Gly (PC_2; M_m 539.6, AnaSpec, San Jose, CA, USA), γ-(Glu-Cys)$_3$-Gly (PC_3; M_m 771.9, AnaSpec), γ-(Glu-Cys)$_4$-Gly (PC_4; M_m 1004.1, AnaSpec), γ-(Glu-Cys)$_2$-Ala (hPC_2; M_m 553.6, GenScript Corporation), γ-(Glu-Cys)$_3$-Ala (hPC_3; M_m 785.9, Peptide 2.0 Inc., Chantilly, VA, USA), and γ-(Glu-Cys)$_4$-Ala (hPC_4; M_m 1018.2, Peptide 2.0 Inc.) were prepared in analytical-grade type I water (Milli-Q Synthesis, Millipore). Aliquots of the stock solutions were immediately frozen in liquid N_2, lyophilized and stored at –80 °C. A 30 mM $HgCl_2$ (Merck, Darmstadt, Germany) stock solution was prepared in Milli-Q water, protected from light and stored at room temperature. Hg–biothiol complexes standard solutions were prepared just before usage by mixing appropriate amounts of Hg and biothiol stock standard solutions at different ratios (in μM; 25:50, 50:50, and 50:25) in 0.1% (v/v) of formic acid (50%; Sigma-Aldrich).

Biothiol and Hg–biothiol analysis by HPLC-ESI-TOFMS

Chromatographic separation was performed with an HPLC system (Alliance 2795, Waters, Milford, MA, USA) following the procedure described by Rellán-Álvarez *et al*. (2006b) with some modifications. A reverse-phase monolithic column (Chromolith Performance RP-18e, 3 × 100 mm, Merck, Darmstadt, Germany) was used. Injection volume was 50 μL for standard solution and 20 μL for root SF. Autosampler and column compartment temperatures were kept at 6 and 30 °C, respectively. The mobile phase was built using three eluents: A (Milli-Q water), B (acetonitrile) and C (2% formic acid in water), all chemicals being HPLC-MS grade (Riedel-de Haën, Seelze, Germany). Samples were eluted (flow rate of 400 μL min^{-1}) with a gradient program: the initial conditions (95% A, 0% B and 5% C; min 0) were linearly changed to 85% A, 10% B and 5% C until min 5, and then changed to 45% A, 50% B and 5% C until min 6. After that, an isocratic step with the latter composition was applied until min 9. Then, to return to the initial conditions, a new linear gradient to 95% A, 0% B and 5% C was run until min 11, followed by a 4 min re-equilibration. The exit flow from the column was split with a T-connector (Upchurch Scientific, Oak Harbor, WA, USA) that directed *a.* 200 μL min^{-1} into the

electrospray ionization (ESI) interface of a time-of-flight mass spectrometer (TOFMS) micrOTOF II (Bruker Daltonics, Bremen, Germany). The TOFMS operated in negative ion mode at –500 and 3000 V of endplate and spray tip voltages, respectively. The orifice voltage was set at –90 and –150 V to acquire spectra in the mass-to-charge ratio (m/z) ranges of 50–1000 and 900–3000, respectively. In positive ion mode, endplate and spray tip voltages of –500 and 4500 V were used. The orifice voltage was set at 100 and 270 V to acquire spectra in the 50–1000 and 900–3000 m/z ranges, respectively. The nebulizer gas (N_2) pressure, drying gas (N_2) flow rate and drying gas temperature were 1.6 bar, 7.9 L min^{-1} and 180 °C. The mass axis was calibrated externally using Li-formate adducts (10 mM LiOH, 0.2% (v/v) formic acid and 50% (v/v) 2-propanol). The HPLC-ESI-TOFMS system was controlled with the software packages MicrOTOF Control v.2.2 and HyStar v.3.2 (Bruker Daltonics). Data were processed with Data Analysis v.3.4 (Bruker Daltonics). Ion chromatograms were extracted with a precision of ±0.05 m/z units.

Synchrotron X-ray fluorescence microprobe (μ-SXRF) and X-ray computed micro-tomography (SR-μCT)

Three-week-old *M. sativa* primary roots were further analysed by microprobe at beamline 2–3 at the Stanford Synchrotron Radiation Lightsource (SSRL). μ-SXRF mapping of Hg was collected by scanning a representative intact root in the microfocused beam at 13 500 eV sampled in 2 × 2 μm pixels. Samples were rinsed several times with 10 mM Na_2 EDTA solution to remove Hg adhered to the root surface. Roots were then freeze-dried to preserve root tissue, placed in large (~3 × 3 cm) Al spacers bound with kapton tape, and stored at room temperature until analysis. The Kα fluorescence line intensities of Hg (and other elements of interest, such as S) were measured with a three-element Ge detector and normalized to the incident monochromatic beam intensity. $HgCl_2$ powder was used as a standard material for calibration. Fluorescence micro-tomography data were collected as a function of a X-axis position and a rotation angle using 3 μm translation step, 1° angular step and dwell times of 125 ms, resulting in a fluorescence sinogram image. Data analysis was carried out with the software package SMAK version 0.45 (Webb 2005).

Extended X-ray absorption fine structure (EXAFS)

Firstly, Hg–biothiol standards were prepared in a 2:1 ratio (ligand:Hg) in Mili-Q water, mixing (1) pure hPCs (hPC_2, hPC_3 or hPC_4) (2 mM) and $HgCl_2$ (1 mM); (2) PCs (PC_2, PC_3 or PC_4) (0.5 mM) and $HgCl_2$ (0.25 mM); and (3) GSH or hGSH (4 mM) and $HgCl_2$ (2 mM). The aqueous solutions of Hg–biothiol complexes were mixed with 25% v/v glycerol to prevent the formation of ice crystals. The standard mixture was stored under liquid nitrogen until analysis. Spectra from the additional standard compounds: Hg (II) cysteine ligand (average of mercury cysteine and dicysteine), Hg acetate (HgAce), cinnabar (HgS red), metacinnabar (HgS black), methyl-Hg aspartate (MeHgAsp) and methyl-Hg methionine (MeHgMet) were also used for fit calculations (details can be found in Rajan *et al*. 2008). Hg L_3 edge X-ray absorption spectra for the hydroponic *M. sativa* root (average of five scans) and for the standard mixtures (average of three scans) were collected at beamline 9-3 at SSRL by monitoring the Hg $L_{\alpha 1}$ fluorescence at 9988 eV. The tissue sample was ground in liquid nitrogen and placed in aluminium spacers. A 200 μL aliquot of the aqueous standard solution was placed in a Lucite sample holder. All samples were bound by kapton tape and stored in liquid nitrogen. During the analysis, the samples were maintained at ≈10 °K in a liquid helium flow cryostat and positioned at 45° to the incident beam. Calibration was accomplished by simultaneous collection of $HgCl_2$ with first-edge inflection at 12 284.4 eV. Data analysis was carried out with the software package SixPACK version 0.63 (Webb 2005) following a standard method that consisted of preliminary examination of fluorescence channels and energy calibration of individual scans using a smoothed first derivative, followed by data averaging. A linear background function was subtracted, and data were normalized to a unit step edge. To quantify the percentage of each Hg species present in alfalfa roots using the fingerprinting method, a least squares fit (LSF) was performed to fit the EXAFS (*chi*) of the experimental data to linear combinations of standard reference compounds, which were divided into four Hg coordination environments: inorganic sulphur bonding (Hg–S red and Hg–S black), organic sulphur bonding (Hg–PCs and Hg–Cys), oxygen-rich ligand bonding (carboxylic groups) (Hg–Ace) and methyl-Hg forms (Me-Hg–Asp and Me-Hg–Met). Single-component fits to the data were carried out to exclude those contributing less than 1%, and selected candidates of each group were fitted to get the relative proportion of Hg species. The reduced *chi*-square value (goodness of fit χ^2) provides information as to the quality of the standard fit to the spectra data (Kim *et al*. 2000).

Statistical analysis

Statistical significance was calculated by the Duncan's test of analysis of variance (at $P < 0.05$), using the SAS statistical software package.

RESULTS

Plant growth and Hg distribution in tissues

The growth of roots was not affected significantly in plants treated with 30 μM Hg for 7 d in a semi-hydroponic culture (Table 1), and no visual symptoms of toxicity appeared. Total root Hg concentrations were approximately 1600, 500 and 800 μg g^{-1} FW in barley, maize and alfalfa plants treated with Hg, respectively, whereas control plants had Hg

Table 1. Fresh weight (mg plant^{-1}), and total and subcellular Hg concentration (μg g^{-1} fresh weight) of roots from 3-week-old barley, maize and alfalfa plants treated with 0.0 (control) or 30 μM Hg (+Hg) for 7 d. In parentheses, the percentage of Hg distribution relative to the total is shown. Particulate Fraction, PF; Microsomal Fraction, MF; Soluble Fraction, SF. Data are average of three independent replicates (±SD). Data for MF and SF were originally measured on a total metal basis and then transformed into a μg g^{-1} fresh weight basis

	Root fresh weight		[a]Hg concentration					
	Control	+Hg	Total	PF		MF[b]	SF	
Barley	21 ± 9	24 ± 7	1599 ± 217	1047 ± 222	(66)	<0.03	1.01 ± 0.06	(0.06)
Maize	118 ± 27	102 ± 25	517 ± 40	320 ± 121	(61)	<0.03	0.32 ± 0.02	(0.06)
Alfalfa	500 ± 204	440 ± 133	816 ± 184	757 ± 36	(92)	<0.03	0.69 ± 0.01	(0.08)

[a]Mercury concentration in roots and subcellular fractions from control plants were below detection limits.
[b]Only traces of Hg (slightly below the quantification limit) were found in the microsomal fraction.

concentrations below the detection limit (<0.05 μg g^{-1} FW). Shoot Hg concentration values were only approximately 2% of those found in roots (data not shown), in agreement with the known allocation of this toxic metal in plants grown under similar conditions (Sobrino-Plata *et al*. 2009; Válega *et al*. 2009). Therefore, we focused on Hg fractionation, speciation and allocation in root tissues.

Subcellular fractionation and association of soluble Hg with biothiols in roots

Three subcellular fractions were isolated from root tissue: a particulate (PF), a microsomal (MF) and a soluble fraction (SF), and the Hg concentration of each fraction were measured. The vast majority of Hg (approximately 99.9% in barley, maize and alfalfa) was found associated with the PF, which contains mainly cell walls (Table 1). A much smaller portion (approximately 0.1% in all cases) of Hg was found in the SF, whereas the Hg detected in the MF was just below the quantification limit (below 0.01%). Mercury concentrations were in the SF equivalent to approximately 1.0, 0.3 and 0.7 μg g^{-1} FW of barley, maize and alfalfa, respectively. Anion exchange DEAE-chromatography of SF revealed that Hg co-eluted with a peak containing most of the biothiols from maize root SF (Fig. 1); the amount of Hg recovered represents approximately 70% of the total Hg SF.

Detection of Hg–biothiol complexes by HPLC-ESI-TOFMS

Mass spectrometry-based analyses were carried out to identify the Hg species occurring in root SF, using an approach similar to that used recently by Krupp *et al*. (2008, 2009) and Chen *et al*. (2009). Hg–containing compounds were identified by the characteristic natural Hg isotopic composition (^{196}Hg, ^{198}Hg, ^{199}Hg, ^{200}Hg, ^{201}Hg; ^{202}Hg, and ^{204}Hg) using ESI-TOFMS (Chen *et al*. 2009). An array of biothiol and Hg–biothiol standard solutions was used to establish the HPLC-ESI-TOFMS analytical conditions, prepared at three concentration ratios (1:2, 1:1 and 2:1), with the following ligands: GSH, hGSH (γ-Glu-Cys)$_2$ (GC_2) (γ-Glu-Cys)$_2$-Gly (PC_2) (γ-Glu-Cys)$_2$-Ala (hPC_2) (γ-Glu-Cys)$_3$-Gly (PC_3), and (γ-Glu-Cys)$_3$-Ala (hPC_3). Acidic chromatographic conditions were used, similar to those established for the determination of reduced and oxidized GSH and hGSH (Rellán-Álvarez *et al*. 2006b), based on the fact that Hg–biothiol complexes are stable at pH 2.0 (Chen *et al*. 2009). Most biothiol ligands and Hg–biothiol complexes were detected both in negative and positive ionization. Because the ionization polarity could affect sensitivity to detect each Hg–biothiol complex, positive and negative ionizations were always used. Moreover, to detect the full array of possible Hg–complexes, TOFMS mass spectra were acquired in two different mass-to-charge ratio (m/z) ranges: 100–1000 and 1000–3000. Therefore, a total of four individual HPLC-ESI-TOFMS runs were carried out per sample (negative and positive mode, in two mass-to-charge ratios each), with high-resolution mass spectra acquired to obtain three-dimensional (time, m/z and intensity) chromatograms.

The ion chromatograms of free biothiols were extracted at the exact m/z-values of the $[M+H]^+$ and $[M–H]^-$ ions corresponding to the monoisotopic signals (Fig. 2a), and the ion chromatograms of Hg–biothiol complexes (Fig. 2b and 2c) were extracted at the exact m/z-values of the $[M+H]^+$ and $[M–H]^-$ ions corresponding to the ^{202}Hg

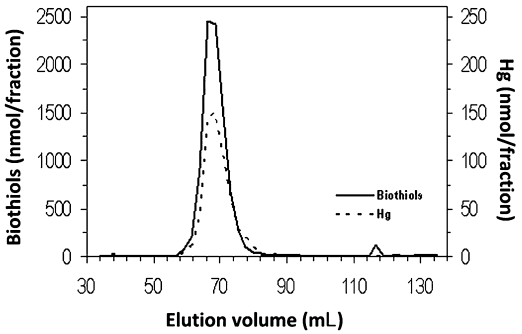

Figure 1. FPLC-DEAE anion exchange chromatography of the soluble fraction from maize roots treated with 30 μM Hg. Samples collected were analysed for biothiols reacting with Ellman's reagent (continuous line) or for Hg (dashed line) and plotted against elution volume. Data are representative of three independent experiments.

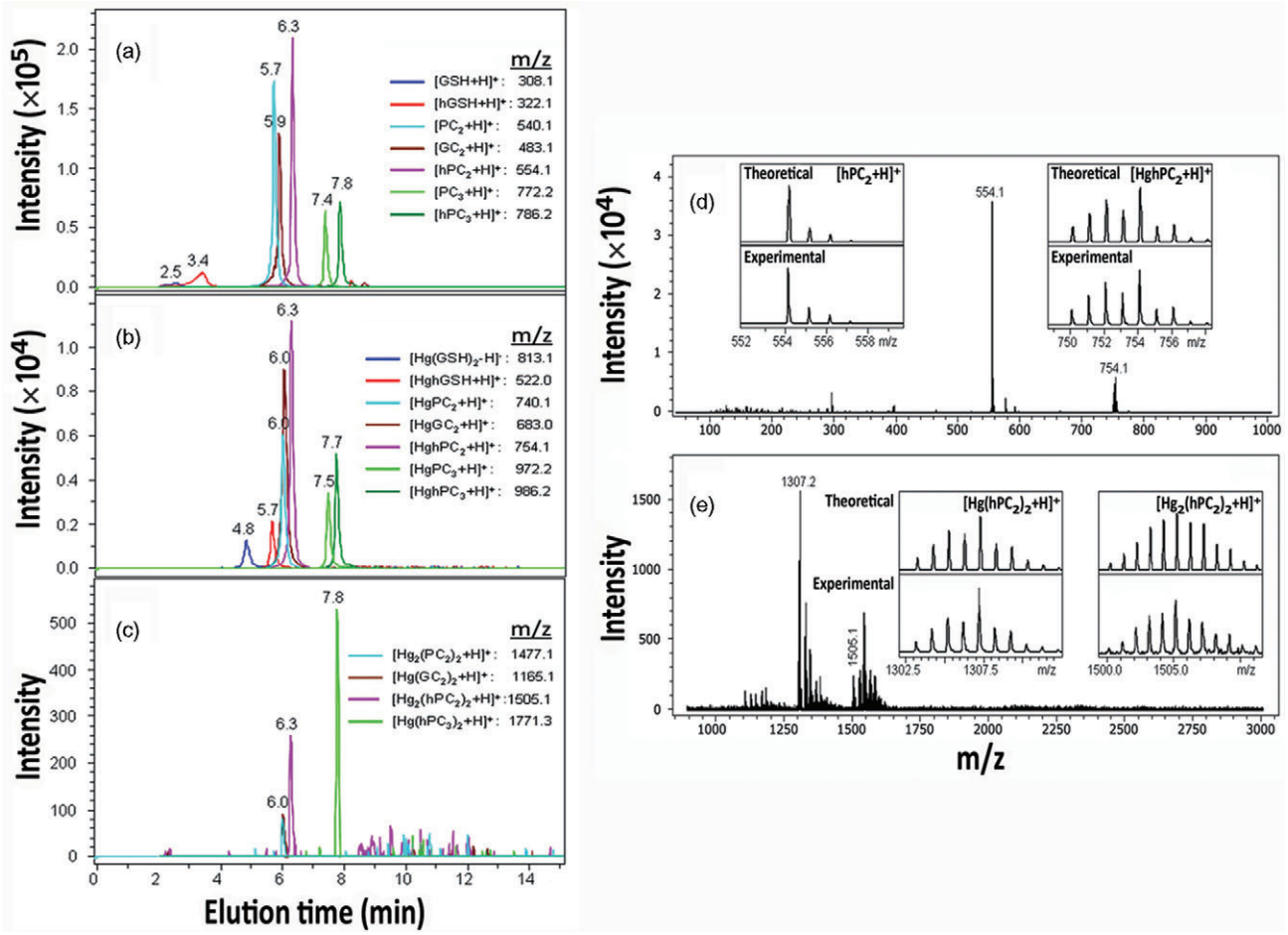

Figure 2. HPLC-ESI-TOFMS analysis of biothiol ligands (50 μM) and Hg-biothiol complexes (mixture of Hg:biothiol; 25 μM:50 μM) standard solutions in 0.1% formic acid. Peaks corresponding to different biothiol ligands (a) and Hg-biothiol complexes of low *m*/*z* (50–1000 range; b) and high *m*/*z* (900–3000 range; c) are shown. Mass spectra of a Hg:hPC_2 mixture standard solution (25:50 μM in 0.1% formic acid) acquired in the 50-1000 (d) and 900–3000 (e) *m*/*z* ranges. Experimental and theoretical isotopic signatures of the identified ions are shown in insets.

(most abundant isotope) signal. Results show that the HPLC-ESI-TOFMS method adequately resolved free biothiols and Hg–biothiol complexes (Fig. 2). Differences in retention times between the free and Hg–complexed biothiols were only found in the case of small biothiols such as GSH and hGSH. For instance, GSH eluted at 2.5 min (Fig. 2a) whereas $Hg(GSH)_2$ eluted at 4.8 min (Fig. 2b). Figure 2d shows an example of ESI-TOFMS spectra in the positive mode of one of the standards tested (Hg:hPC_2; 25:50 μM). When data were acquired in the 100–1000 *m*/*z* range, two main ions at *m*/*z* 554.1 and 754.1 were found. A close-up of the mass spectrum of the ion at *m*/*z* 554.1 shows that it corresponds to free $[hPC_2+H]^+$ (inset in Fig. 2d). However, the ion at *m*/*z* 754.1 and isotopic signature fit well with a single charged ion containing one Hg atom complex ($[HghPC_2+H]^+$; inset in Fig. 2d). When mass spectra were acquired in the 1000–3000 *m*/*z* range, two further ions at *m*/*z* 1307.2 and 1505.1 were found (Fig. 2e), with signal intensities one order of magnitude lower than that of $[HghPC_2+H]^+$. The ion at *m*/*z* 1307.2 had an isotopic signature characteristic of a single charged ion containing one Hg atom, and the *m*/*z* fit well with $[Hg(hPC_2)_2+H]^+$. The ion at *m*/*z* 1505.1 showed an isotopic signature characteristic of a single charged ion containing two Hg atoms, and the *m*/*z* fit well with $[Hg_2(hPC_2)_2+H]^+$ (Fig. 2e). The existence of two or more Hg atoms changes the fingerprint of the complex, as observed by comparing the isotopic signatures of $[Hg(hPC_2)_2+H]^+$ and $[Hg_2(hPC_2)_2+H]^+$ ions. A wide array of Hg–biothiol complexes was found in standard solutions prepared at three Hg-to-biothiol concentration ratios (1:2; 1:1 and 2:1) by HPLC-ESI-TOFMS. The *m*/*z* and retention time values of all free biothiol and Hg–biothiol ions detected are presented in Supporting Information Table S1. Independent of the proportions of Hg and PCs used in the standard preparation, the most frequent Hg–biothiol ions found corresponded to Hg–complexes with a 1:1 stoichiometry. Phytochelatins with a higher number of sulfhydryl residues such as PC_3 and hPC_3 also formed complexes with higher stoichiometries (4:2 or 2:1 Hg:ligand) in the case of the Hg-richest mixtures (e.g. the

$[Hg_4(hPC_3)_2\text{-}2H]^{2-}$ ion; Supporting Information Table S1). These heavily Hg-loaded complexes showed higher retention times than those of Hg–biothiol complexes with lower stoichiometries.

When the root SF of alfalfa, maize and barley plants treated with 30 μM Hg was analysed using HPLC-ESI-TOFMS, a total of 28 Hg-containing ions were detected corresponding to 17 different Hg–complexes (ions were detected in positive mode, negative mode or in both), formed with up to six different biothiols (GC_2, PC_2, hPC_2, hPC_3, PC_4, and hPC_4; summarized in Table 2). Fourteen of the 17 Hg-containing complexes were unequivocally identified based on retention time, exact *m*/*z*, and isotopic signature (see fits between experimental and theoretical isotopic signatures in Supporting Information Fig. S1). In barley, three 1:1 Hg–complexes were found, one each with GC_2, PC_2 and PC_4. In maize, Hg formed only two complexes with GC_2, having 1:1 and 2:2 stoichiometry. In alfalfa, up to 14 different Hg–biothiol complexes were found, one each with GC_2 ($HgGC_2$) and PC_2 ($HgPC_2$), four with hPC_2 ($HghPC_2$, $Hg(hPC_2)_2$, $Hg_2(hPC_2)_2$ and $Hg_3(hPC_2)_3$), three with hPC_3 ($HghPC_3$, $Hg(hPC_3)_2$ and $Hg_2(hPC_3)_2$), two with hPC_4 ($HghPC_4$ and Hg_2hPC_4), and two more with PC_4 ($HgPC_4$ and Hg_2PC_4). Additionally, we could detect a complex formed with methyl-Hg and hPC_2 (CH_3-Hg–hPC_2) in alfalfa SF, not previously described in the literature. Therefore, the most abundant Hg-to-ligand stoichiometry found was 1:1. Moreover, some of the Hg–biothiol complexes having thiol groups not bound to Hg were found to occur in oxidized forms ($Hg(hPC_{2ox})_2$, $Hg(hPC_{3ox})_2$, $Hg_2(hPC_{3ox})_2$ and $Hg(hPC_{4ox})$, and eluted with a delay of approximately one min as compared with their reduced counterparts. Finally, three more Hg-containing ions were found in alfalfa at *m*/*z* 1084.2, 1165.2 and 1834.3, which could not be identified (Table 2).

As an example, some chromatographic and MS data obtained for the three plant species are shown in Fig. 3. Barley root SF showed (in positive mode) two single charged ions containing one Hg atom at *m*/*z* 683.1 and 740.1, both eluting at 6.2 min, that had *m*/*z* and isotopic signatures matching those of $[HgGC_2H]^+$ and $[HgPC_2+H]^+$ ions, respectively (Fig. 3a). Maize root SF only showed two single charged Hg-containing ions, at *m*/*z* 683.1 (in positive mode) and 1361.2 (in negative mode), eluting at 6.2 min and with *m*/*z* and isotopic signatures fitting well with those of $[HgGC_2+H]^+$ and $[Hg_2(GC_2)_2\text{-}H]^-$ ions, respectively (Fig. 3b). Alfalfa root SF showed (in negative mode) two single charged ions containing one Hg atom, at *m*/*z* 1503.2

Table 2. Mercury-containing ions detected in positive and negative mode HPLC-ESI-TOFMS analysis of root soluble fractions from 3-week-old barley, maize, and alfalfa plants treated with 30 μM $HgCl_2$ for 7 d. The identification of the ions detected along with their mass-to-charge ratio (*m*/*z*) and chromatographic retention times (t_R; in minutes) are indicated. Data were obtained from 3 independent biological replicates

Plant species	Formula species complex	t_R	Ion positive mode	Ion negative mode	*m*/*z*
Barley	Hg-GC_2	6.2	$[HgGC_2+H]^+$		683.1
		6.2		$[HgGC_2–H]^-$	681.1
	Hg-PC_2	6.3	$[HgPC_2+H]^+$		740.1
		6.3		$[HgPC_2–H]^-$	738.1
	Hg-PC_4	8.3		$[HgPC_{4ox}–H]^-$	1200.2
Maize	Hg-GC_2	6.2	$[HgGC_2+H]^+$		683.1
		6.2		$[HgGC_2–H]^-$	681.1
	Hg_2-$(GC_2)_2$	6.2		$[Hg_2(GC_2)_2–H]^-$	1361.2
Alfalfa	CH_3-Hg-hPC_2	6.0		$[CH_3HghPC_2–H]^-$	768.1
	Hg-GC_2	6.2		$[HgGC_2–H]^-$	681.1
	Hg-PC_2	6.2		$[HgPC_2–H]^-$	738.1
	Hg-*Unknown*	6.7		[Hg *Unknown*]$^-$	1084.2
		6.7		[Hg *Unknown*]$^-$	1165.2
		6.7		[Hg *Unknown*]$^-$	1834.3
	Hg-hPC_2	6.8	$[HghPC_2+H]^+$		754.1
	Hg_2-$(hPC_2)_2$	6.8		$[Hg_2(hPC_2)_2–H]^-$	1503.2
	Hg_3-$(hPC_2)_3$	6.8		$[Hg_3(hPC_2)_3–H]^-$	2255.3
	Hg-$(hPC_{2ox})_2$	7.7	$[Hg(hPC_{2ox})_2+;2H]^{2+}$		653.1
		7.7	$[Hg(hPC_{2ox})_2+H]^+$		1305.2
	Hg-hPC_3	8.0		$[HghPC_3–H]^-$	984.2
	Hg-PC_{4ox}	8.3	$[HgPC_{4ox}+H]^+$		1202.2
		8.3		$[HgPC_{4ox}–H]^-$	1200.2
	Hg-hPC_{4ox}	8.3	$[HghPC_{4ox}+H]^+$		1216.2
		8.3		$[HghPC_{4ox}–H]^-$	1214.2
	Hg-$(hPC_{3ox})_2$	8.4	$[Hg(hPC_{3ox})_2+H]^+$		1767.3
	Hg_2-$(hPC_{3ox})_2$	8.4	$[Hg_2(hPC_{3ox})_2+H]^+$		1967.3
	Hg_2-PC_{4ox}	8.5		$[Hg_2PC_{4ox}–H]^-$	1400.2
	Hg_2-hPC_{4ox}	8.5		$[Hg_2hPC_{4ox}–H]^-$	1414.2

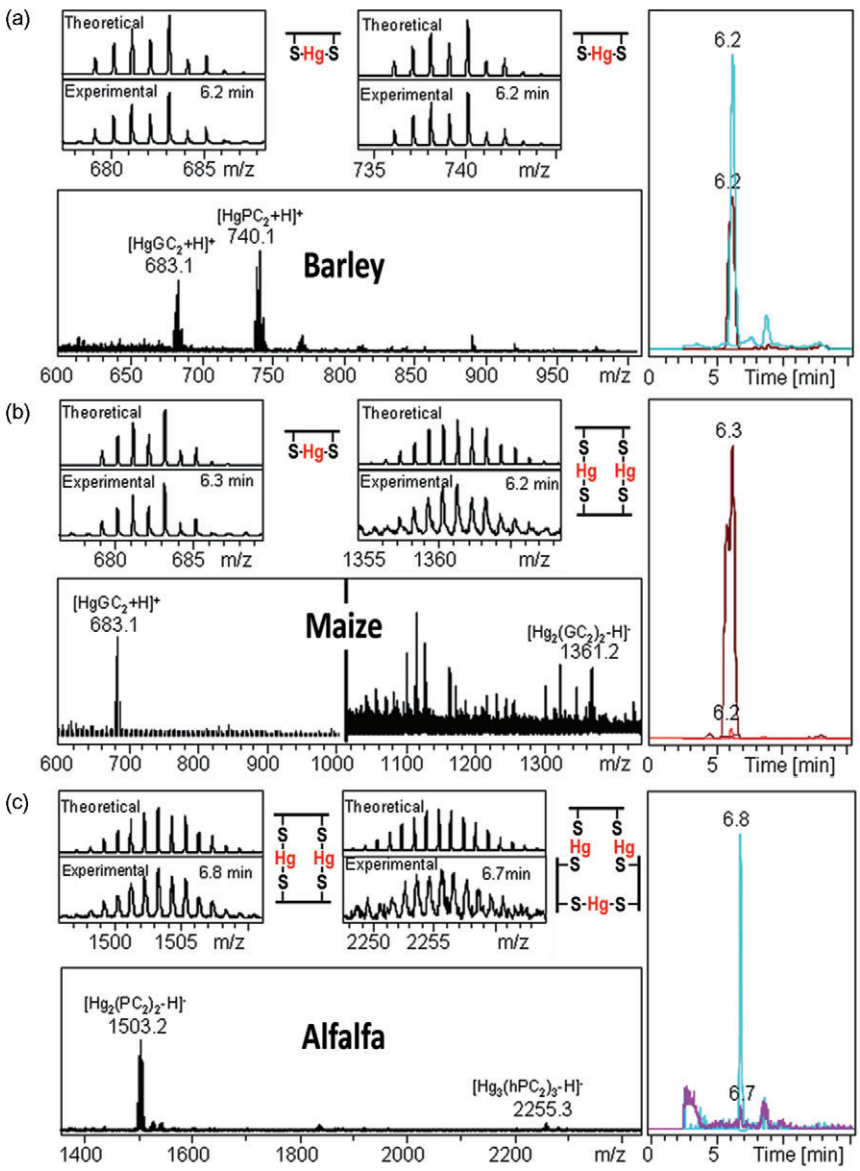

Figure 3. Analysis of some Hg-phytochelatin complexes found in the root soluble fraction of 3-week-old barley (a), maize (b), and alfalfa (c) plants treated with 30 μM $HgCl_2$ for 7 d. HPLC-ESI-TOFMS analyses were carried out in negative and positive modes, and data were acquired at different *m*/*z* ranges. On the left panels, chosen mass spectra extracted at the retention times indicated in the chromatograms shown on the right panels are displayed. Insets highlight experimental and theoretical isotopic signatures of the identified ions as well as a schematic diagram of the putative Hg-S bonds.

(at 6.8 min) and 2255.3 (at 6.7 min), that were identified as $[Hg_2(hPC_2)_2\text{-}H]^-$ and $[Hg_3(hPC_2)_3\text{-}H]^-$, respectively (Fig. 3c).

In vivo X-ray spectroscopy of Hg in alfalfa roots

The spatial localization of Hg and S was studied in alfalfa roots treated with 30 μM Hg using μ-SXRF (Fig. 4a and 4b). The most intense Hg signals were found in the inner tissues, possibly at the vascular cylinder. At this location, there was significant overlap with Hg and sulphur (S; Fig. 4b; see overlay in Fig. 4c). The correlation between intensities of Hg and S was highly significant (r^2 of 0.84; see Supporting Information Fig. S2). To confirm the distribution of Hg found in primary alfalfa roots, an analysis with enhanced 2D spatial resolution was performed using computed micro-tomography (SR-μCT). Both longitudinal (Fig. 4d) and transversal (Fig. 4e) imaging showed that the strongest Hg signals were detected in the vascular cylinder, with less signal evident in the epidermis, in agreement with the μ-SXRF data (Fig. 4a).

To undertake the *in vivo* speciation of Hg in roots of 30 μM Hg-treated alfalfa plants, we performed XAS, which permits non-disruptive analysis in frozen root material. Confidence in the accuracy of the fit was increased by using a diverse standard library, taking into account the most probable Hg coordination environments in plants, since the goodness of the LSF approach depends on the standard compounds selected a *priori* (Beauchemin, Hesterberg & Beauchemin 2002). A first LSF was performed in each group of standard mixtures (inorganic sulphur-Hg forms, biothiol and cysteine Hg ligand bonding, oxygen-rich ligand bonding and methyl-Hg forms) in order to exclude those standard compounds contributing less than 5% in the fit.

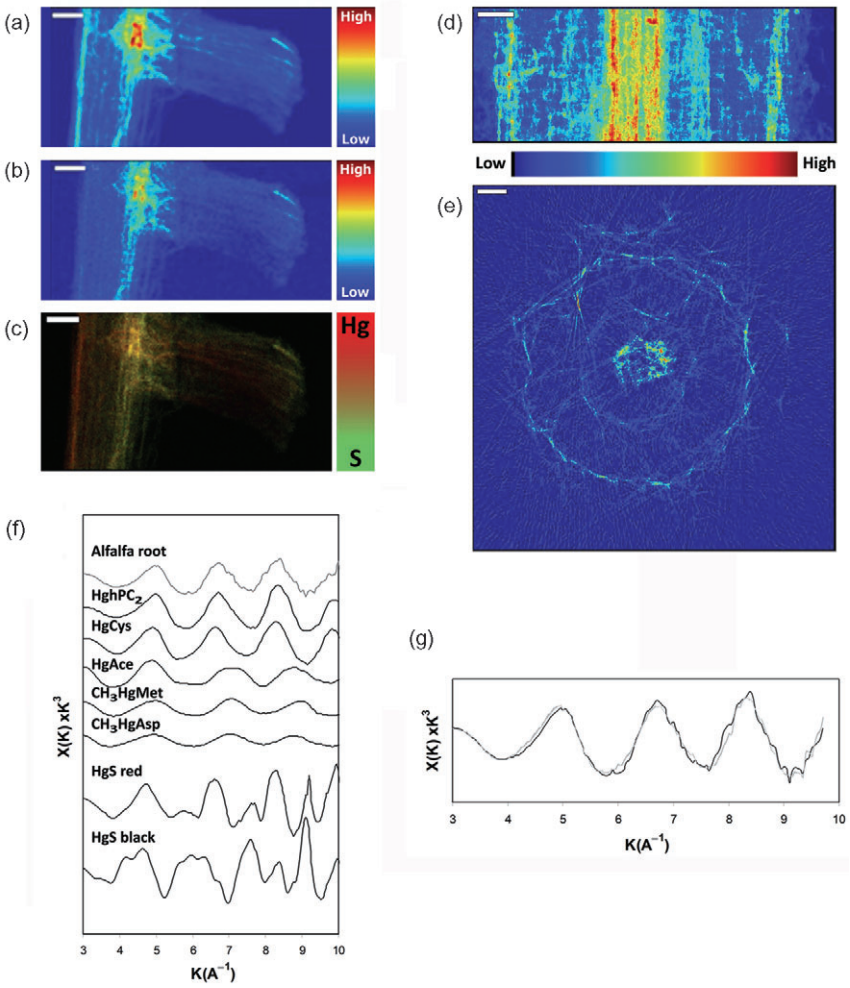

Figure 4. X-ray spectroscopy to study Hg distribution and ligand association in three-week-old *Medicago sativa* roots treated with 30 μM Hg for 7 d in a pure-hydroponic system. (a) Elemental 2-D SXRF distribution of Hg; (b) distribution of sulphur; and (c) overlapping of Hg (red) and S (green); white scale bars equal 50 μm. (d) Longitudinal section showing Hg spatial distribution of primary root. (e) Micro-tomography of the same primary root showing a transversal analysis of Hg localization; white scale bars equal 100 μm. (f) Hg L_3 EXAFS spectra of the Hg model compounds plus alfalfa root. (g) Linear fitting results for alfalfa root (black line: data, gray line: fit), showing the Hg L_3 EXAFS k^3 weighted spectra (reduced *chi*-square 0.0909). The components that contributed to the linear fit were HgCys (33.8%), HghPC (45.2%) and MeHgMet (21%).

This preliminary survey showed that the spectra of the different HgPCs, and also the HgCys complexes were indistinguishable from each other. Therefore, we opted to use $HghPC_2$ and HgCys as representative standards for Hg–biothiol or Hg–organic sulphur (also protein) complexes. The Hg L_3 EXAFS spectra of the Hg model compounds plus the current sample are shown in Fig. 4d. Organic Hg–S coordination (HgCys and $HghPC_2$) and methyl-Hg forms (MeHgMet) accounted for 79% and 21%, respectively, of the total Hg in alfalfa roots (reduced *chi*-square 0.0909). The best LSF of the EXAFS spectra to the standards HgCys, HghPC and MeHgMet that represents the different Hg forms in alfalfa roots is shown in Fig. 4e.

Tolerance analysis of *A. thaliana cad1-3* and *cad2-1* mutants

To evaluate the relevance of Hg–PC complex formation for Hg detoxification and tolerance root growth inhibition, a biothiol profile was studied in *A. thaliana* mutants with altered biothiol metabolism. *cad2-1* and *cad1-3* mutants were clearly less tolerant than the wild-type when exposed to 10 μM Hg for 4 d: root growth inhibition was over 80% in the mutants, whereas WT was inhibited by only 35% (Fig. 5). The biothiol profile of each plant was analysed by conventional HPLC in leaves infiltrated with 30 μM Cd or Hg for 48 h (Supporting Information Fig. S3). Cd-treated leaves of *cad2-1* mutants accumulated a lower amount of GSH (40%) and PCs (<31%) than Col-0, and no PCs were detected in leaves exposed to 30 μM Hg (Table 3). As expected, *cad1-3* did not accumulate PCs under Cd nor Hg stress, although a remarkable increase in GSH level was detected, over 150% the concentration found in Col-0 (Table 3). HPLC-ESI-TOFMS analysis revealed that Hg–PC_2 complexes were only detected in Col-0 leaves ($[HgPC_2+H]^+$), whereas no traces of Hg–biothiol complexes could be detected in *cad2-1* or in *cad1-3* (data not shown). HPLC-ESI-TOFMS sensitivity was checked by the addition of Hg–GSH spikes to Col-0 leaves infiltrated with 30 μM Hg. We could only detect $[Hg(GSH)_2–H]^-$ at *m/z* 813.1 with the highest spike concentration (25 μM Hg:50 μM GSH; Supporting Information Fig. S4B), whereas this ion was not detected in Col-0 leaves spiked with 2.5 μM Hg:5 μM GSH (Supporting Information Fig. S4C) nor in non-spiked 30 μM Hg-treated leaves (Supporting Information Fig. S4D).

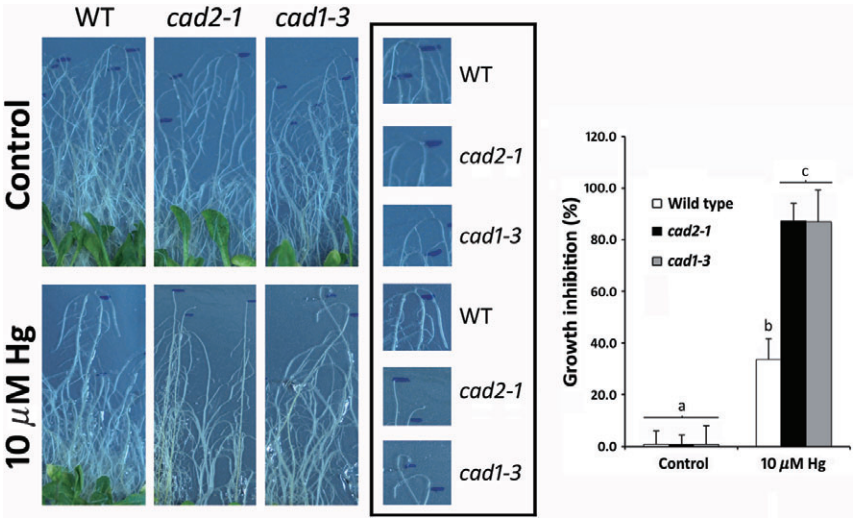

Figure 5. Tolerance to Hg assay with *Arabidopsis thaliana* mutants altered in biothiol metabolism: Wild-type (Col-0), *cad2-1* (altered γ-glutamyl cysteine synthase activity), and *cad1-3* (lacking PCS activity). Seven-day-old seedlings were turned roots-up and exposed to control (0) or 10 μM Hg by placing a 3MM filter paper strip close to the root apical tip. Close-ups of the root tips (insets in black rectangle) highlight the remarkable sensitivity of both mutants compared with the WT. Outgrowth root length was measured from the blue mark and growth inhibition calculated after 5 d exposure (see graph on the right). Results are the average of 10 replicates, and different letters denote significant differences with $P < 0.05$.

DISCUSSION

Although plants examined in this study were treated with a high dose of Hg (30 μM), they were not poisoned and effective defence mechanism(s) were exerted in agreement with our previous results (Sobrino-Plata *et al*. 2009). Roots were the major sink for Hg, as already described in these plant species (Rellán-Álvarez *et al*. 2006a; Sobrino-Plata *et al*. 2009). Several subcellular fractions were prepared from roots of Hg-treated alfalfa, maize, and barley plants. The largest amount of Hg accumulated in the root PF (up to 99%), with the SF representing a secondary pool, was in agreement with the distribution described in *Halimione portulacoides* using a similar experimental approach (Válega *et al*. 2009). Retention of heavy metals by materials associated with the cell wall and/or via complexation in the intracellular space have been described as important tolerance mechanisms to avoid its accumulation in cytosol and organelles (Hall 2002). Thus, Hg has been found associated with the cell wall of different plant species (*Pisum sativum* and *Mentha spicata*, Beauford *et al*. 1977; *Nicotiana tabacum*, Suszcynsky & Shann 1995). The chromatographic separation of maize SF by DEAE-FPLC revealed that the major proportion of soluble Hg was associated with biothiols, which agrees with the reported recovery of Cd in maize (Rauser & Meuwly 1995) and *Sedum alfredii* (Zhang, Chen & Qiu 2010) after a similar chromatographic separation of soluble Cd. These results highlight the relevance of biothiol ligands in Hg speciation in plants.

To identify the biothiol ligands involved in Hg complexation, root SFs of barley, maize and alfalfa plants exposed to 30 μM Hg were analysed in depth by HPLC-ESI-TOFMS. The HPLC-ESI-TOFMS analysis of the root SF of barley, maize and alfalfa plants exposed to 30 μM Hg revealed that Hg was only found associated with PCs. No other Hg-containing substances were identified with our experimental settings, although other bioligands such as organic acids, nicotianamine or amino acids can be important in metal homeostasis (Sharma & Dietz 2006). A wide array of Hg–PC complexes was found: three in barley, two in maize

Table 3. Concentration of biothiols (nmol g^{-1} FW) in *Arabidopsis thaliana* leaves infiltrated with 30 μM Cd or Hg for 48 h. In parentheses is the percentage of concentration relative to wild-type. Values are the mean of four independent replicates ± standard deviation ($P < 0.05$)

Biothiol	Wild type	*cad2-1*	*cad1-3*
Control			
Cys	$23.4^{a} \pm 4.8$	$21.5^{a} \pm 4.7$ (92)	$22.6^{a} \pm 9.7$ (96)
GSH	$153.8^{a} \pm 8.4$	$50.1^{b} \pm 10.3$ (33)	$142.1^{a} \pm 14.3$ (92)
30 μM Cd			
Cys	$19.7^{a} \pm 6.5$	$36.6^{ab} \pm 5.8$ (186)	$46.1^{b} \pm 12.8$(234)
GSH	$142.5^{a} \pm 22.8$	$80.0^{c} \pm 22.4$ (56)	$316.1^{d} \pm 29.9$(222)
PC_2	$168.7^{a} \pm 38.7$	$52.5^{b} \pm 18.9$ (31)	n.d.
PC_3	$346.7^{a} \pm 38.6$	$41.0^{b} \pm 14.7$ (12)	n.d.
PC_4	$283.6^{a} \pm 48.6$	$25.6^{b} \pm 8.8$ (9)	n.d.
PC_5	$73.9^{a} \pm 12.7$	n.d.	n.d.
30 μM Hg			
Cys	$25.0^{a} \pm 3.6$	$44.1^{b} \pm 2.2$ (177)	$65.6^{c} \pm 10.1$(263)
GSH	$175.5^{a} \pm 12.4$	$52.0^{b} \pm 7.2$ (30)	$257.4^{d} \pm 21.9$(147)
PC_2	$60.4^{a} \pm 22.4$	n.d.	n.d.
PC_3	$32.3^{a} \pm 9.3$	n.d.	n.d.

[a]Different letters denote significant differences compared with control wild-type samples.

(one of them also present in barley), and 14 in alfalfa (two of them also present in barley). Ten novel Hg–PCs complexes formed with hPCs were unequivocally identified in alfalfa, a leguminous species capable of synthesizing GSH and hGSH, which has been reported to produce several kinds of PCs and hPCs in the presence of toxic metals, including Hg (Sobrino-Plata *et al*. 2009). The synthesis of hPCs depends apparently on the availability of hGSH as substrate, because phytochelatin synthase (PCS) does not distinguish between GSH or hGSH (Loscos *et al*. 2006).

The most common Hg–PC complexes detected in the three plant species studied were those formed with PCs having two γ-glutamylcysteine units (*i.e.* PC_2, hPC_2 and GC_2; Table 2), although up to 7 different Hg–PC complexes with hPC_3, PC_4 and hPC_4 were also found in alfalfa. Similarly, $HgPC_2$, $HgGC_2$, $Hg(Ser)PC_2$ and $Hg(Glu)PC_2$ were found to accumulate in *O. sativa*, whereas in *M. vulgare* $HgPC_2$, $HgGC_2$ and $Hg(Glu)PC_2$ were found by HPLC-ESI-MS/MS (Krupp *et al*. 2009). Although PC_3 and PC_4 were detected in root tissue extracts from *Brassica napus*, the major pool of biothiols corresponded to PC_2 (Iglesia-Turiño *et al*. 2006). Interestingly, the maize SF only contained the biothiol ligand GC_2, which is essentially in agreement with the findings of Meuwly *et al*. (1995), who reported that monocotyledonous plants such as maize preferentially accumulate GCs or des-Gly-phytochelatins after exposure to Cd.

Among the array of Hg–PC complexes detected in alfalfa, barley and maize, the SF mostly had 1:1 Hg to biothiol stoichiometry, as described in *B. chinensis* (Chen *et al*. 2009) and *O. sativa* and *M. vulgare* (Krupp *et al*. 2009). However, we also found Hg–PC complexes with higher stoichiometry such as 2:1, 2:2 and 3:3, mainly in alfalfa root SF (Table 2). Interestingly, there were several complexes that appeared in oxidized forms, such as $Hg–(hPC_{3ox})_2$ or Hg_2-hPC_{4ox}, that were more hydrophobic due to the loss of H, with an elution time delayed by one min relative to their reduced counterparts (Table 2). Similarly, Rellán-Álvarez *et al*. (2006b) observed that oxidized GSH and oxidized hGSH eluted approximately one minute later than GSH and hGSH. Nevertheless, the signal of the $Hg–hPC_{2ox}$ and $Hg–hPC_{3ox}$ was much weaker than $Hg–hPC_2$ or $Hg–hPC_3$ (Supporting Information Fig. S1). Chen *et al*. (2009) could detect only oxidized free PCs, whereas we could clearly find the free reduced ligands when conducting the experiment at nearly neutral pH and in the presence of reducing substances (data not shown). These precautions together with our enhanced detection capabilities by HPLC-ESI-TOFMS permitted us to detect up to 28 Hg-containing ions, particularly abundant in the alfalfa root SF (Table 2).

It is known that plants can reduce Hg^{2+} and accumulate methyl-Hg (Göthberg & Greger 2006). Spinach plants subjected to 0.2 μM accumulated a relatively low proportion of methyl-Hg in roots and shoots (approximately 0.01% of total Hg), which suggests that some methylation may occur (Greger & Dabrowska 2010). Interestingly, a novel complex formed *in vivo* between methyl-Hg and hPC_2 was detected in the SF of alfalfa root (Table 2), albeit with a low MS signal intensity (Supporting Information Fig. S1). Despite the fact that we could not detect free methyl-Hg, it feasible that methyl-Hg forms readily complexes with PCs, although Krupp *et al*. (2009) could not detect methyl-Hg–PCs complexes in *O. sativa* and *M. vulgare* plants treated with 45 μM CH_3Hg.

The distribution of Hg was studied in alfalfa roots by μ-SXRF and SR-μCT. The most intense Hg signal was located in the inner tissues of the vascular cylinder and in the epidermis and co-localised with S in the inner tissues (Fig. 4). Similarly, Patty *et al*. (2009) observed in Hg-treated *Spartina* spp. root tips that the inner tissues had the strongest signal. A high overlap of Hg and S localization was observed in alfalfa root, indicating that cells accumulating Hg also contained substances rich in S. Cadmium was also found to co-localize with S at the vascular bundle in *A. thaliana* roots (Isaure *et al*. 2006). X-ray fluorescence mapping of As and S in rice grains also showed that both elements were localized in the same embryo region, suggesting that As accumulated preferentially in protein and nutrient rich parts of the grain (Lombi *et al*. 2009). These studies suggest that S-containing metabolites might be important for the detoxification of toxic elements in plants.

Riddle *et al*. (2002) reported that Hg was coordinated mainly to organic S ligands using XANES in *E. crassipes*. In another study, Rajan *et al*. (2008) investigated Hg methylation in *E. crassipes*, and Patty *et al*. (2009) analysed Hg binding in *S. foliosa* and *S. alterniflora.* In both cases, the authors concluded that most of the Hg was bound to S in a form similar to Hg–cysteine, and a smaller part (3–36%) was in a methylated-Hg form. Overall, these results are in agreement with our data because more than 79% of the Hg in alfalfa was found bound to organic S and 21% was methyl-Hg. Within the current technological limits of EXAFS and XANES, HgCys, HgGSH, HghGSH, HgPCs and HghPCs show very similar spectra because all of these compounds are bound to Hg *via* a sulfhydryl cysteine group of the biothiols and/or proteins, comparative spectral analysis that was undertaken for the first time in the present study. The more distant atoms in the molecule have limited influence on spectral properties (Beauchemin *et al*. 2002). These results are in accordance with the detection of CH_3HgHPC_2 by HPLC-ESI-TOFMS in alfalfa root SF, as previously discussed.

The analysis of tolerance with Cd-sensitive *A. thaliana* mutants highlighted the importance of Hg–PC complexes for Hg homeostasis. Plants unable to accumulate PCs under Hg exposure, i.e. *cad2-1* and *cad1-3*, were much more sensitive, in agreement with Ha *et al*. (1999). The *cad2-1* mutant contains a defective γ-glutamylcysteine synthetase, which causes a severe depletion in GSH and PCs concentration upon Cd-stress (Cobbett *et al*. 1998), essentially following the same behaviour as observed under Hg stress (Table 3 and Fig. 5). Interestingly, the concentration of GSH in *cad1-3* leaves was much higher under Cd and Hg stress than in Col-0, following the pattern described by Howden *et al*. (1995). However, no Hg–GSH complexes could be detected in Hg-treated *cad1-3*, in agreement with our previous

observations that neither Hg–GSH nor Hg–hGSH complexes could be found in the SF of barley, maize and alfalfa roots, and with the findings in Hg-treated *B. chinensis*, *O. sativa* and *M. vulgare* (Chen *et al*. 2009; Krupp *et al*. 2009). We tested the sensitivity of our HPLC-ESI-TOFMS method by analysing samples of *A. thaliana* Col-0 spiked with a 25 μM Hg:50 μM GSH mixture, and we observed the characteristic $[Hg(GSH)_2–H]^-$ ion at m/z 813.1. The $Hg(GSH)_2$ complex was not detected *in vivo*, in spite of being the endogenous GSH concentration found in 30 μM Hg-treated Col-0 leaves (257.4 nmol g^{-1} FW) 5-fold higher than the concentration of spiked GSH (Supporting Information Fig. S4). The absence of Hg–GSH complexes could be partially explained by the fact that PCs containing a larger number of sulfhydryl residues than GSH or hGSH will bind Hg more strongly, as Mehra *et al*. (1996) showed *in vitro* by circular dichroism and HPLC-UV/visible spectroscopy. These results imply that despite GSH accumulation under Hg stress, PCs are the biothiols that contribute to Hg detoxification in plants.

Phytochelatins are synthesized by the condensation of a molecule of γ-glutamylcysteine on GSH that could contain the thiol group blocked by the transpeptidase activity of phytochelatin synthase (Vatamaniuk *et al*. 2000). Taking into account the strong affinity of Hg for thiol residues, an alteration of PCs and GSH metabolism catalysed by phytochelatin synthase might explain the restricted variety of PCs or hPCs variants found in plants exposed to Hg in comparison with those treated with Cd or As (Table 3; Cobbett & Goldsbrough 2002; Haydon & Cobbett 2007). In this sense, the absence of $Hg–(GSH)_2$ in all root SF and $Hg–PC_3$ in barley root SF, which should be expected in the canonical series of Hg–biothiol complexes, could also depend on the particular molecular stability (*i.e.* strength of bonds or susceptibility to oxidative modifications) and subcellular compartmentalization (*i.e.* vacuolar sequestration) occurring during the detoxification of Hg. Therefore, future work should be directed to characterize the dynamics of Hg–biothiol complexes formation using isotopic labelling and HPLC-ICPMS to quantify precisely their cellular concentration, information necessary to understand the contribution of each Hg species to detoxification.

In summary, plants accumulated several classes of Hg–PC complexes. Biothiols may constitute a sink of soluble Hg, although the major proportion of the toxic metal was found associated with the particulate fraction. Albeit a minor proportion of plant Hg, Hg–PCs in the SF contribute to the ultimate fate of Hg in plants. It is plausible that Hg is mainly retained in the roots, interacting with cell wall components, and only when this barrier is overridden, soluble Hg binds to biothiols. EXAFS fingerprint fits suggest that the bulk of Hg is associated with thiols or cysteine, corresponding to cysteine-related components (probably proteins), which is in agreement with the data from μ-SXRF. Incidentally, the major structural protein in cell walls is extensin, a highly glycosylated protein which contains several residues of cysteine in a so-called Cys-rich domain (Baumberger *et al*. 2003). Therefore, as most Hg accumulates in the particulate fraction, speciation of Hg in cell wall components could be the major task for future work. The precise contribution of each compartment to the tolerance of plants is still in debate, and more sensitive and accurate techniques are needed to analyse the distribution of Hg at the subcellular level and to quantify the amount of Hg bound to the different ligands that accumulate in the plants.

ACKNOWLEDGEMENTS

The authors are grateful to Prof C. Cobbett (University of Melbourne, Australia) and Prof Ann Cuypers (Hasselt University, Belgium) for providing us *A. thaliana cad1-3* and *cad2-1* mutants, respectively. This work was supported by Fundación Ramón Areces (http://www.fundacionareces.es), the Spanish Ministry of Science and Innovation (AGL2010-15151-PROBIOMET and AGL2007-61948), Comunidad de Madrid (EIADES S2009/AMB-1478), Junta Comunidades Castilla-La Mancha (FITOALMA, PBI07-0091-3644) and the Aragón Government (Group A03). The HPLC-ESI-TOFMS equipment was co-financed with EU FEDER funds. Portions of this research were carried out at the Stanford Synchrotron Radiation Lightsource, through the Structural Molecular Biology Program supported by the Department of Energy, Office of Biological and Environmental Research, and by the National Institute of Health, National Centre for Research Resources, Biomedical Technology Program. We thank Dr FF del Campo, L Arroyo-Mendez, R Rellán-Álvarez, and S. Vazquez for technical advice and S Webb for help with μ-SXRF data collection.

REFERENCES

Aldrich M.V., Gardea-Torresdey J.L., Peralta-Videa J.R. & Parsons J.G. (2003) Uptake and reduction of Cr(VI) to Cr(III) by mesquite (*Prosopis* spp.): chromate-plant interaction in hydroponic and solid media studied using XAS. *Environmental Science Technology* **37,** 1859–1864.

Arruda M.A.Z. & Azevedo R.A. (2009) Metallomics and chemical speciation: towards a better understanding of metal-induced stress in plants. *Annals of Applied Biology* **155,** 301–307.

Baumberger N., Doesseger B., Guyot R., *et al*. (2003) Whole-genome comparison of leucine-rich repeat extensions in *Arabidopsis* and rice. A conserved family of cell wall proteins form a vegetative and a reproductive clade. *Plant Physiology* **131,** 1313–1326.

Beauchemin S., Hesterberg D. & Beauchemin M. (2002) Principal component analysis approach for modeling sulfur K-XANES spectra of humic acids. *Soil Science Society America Journal* **66,** 83–91.

Beauford W., Barber J. & Barringer A.R. (1977) Uptake and distribution of mercury within higher plants. *Physiologia Plantarum* **39,** 261–265.

Chen L., Yang L. & Wang Q. (2009) *In vivo* phytochelatins and Hg-phytochelatin complexes in Hg-stressed *Brassica chinensis* L. *Metallomics* **1,** 101–106.

Cho U.H. & Park J.O. (2000) Mercury-induced oxidative stress in tomato seedlings. *Plant Science* **156,** 1–9.

Clemens S. (2006) Evolution and function of phytochelatin synthases. *Journal Plant Physiology* **163,** 319–332.

Clemens S., Kim E.J., Neumann D. & Schroeder J.I. (1999) Tolerance to toxic metals by a gene family of phytochelatin synthases from plants and yeast. *The Embo Journal* **18,** 3325–3333.

Cobbett C. & Goldsbrough P. (2002) Phytochelatins and metallothioneins: roles in heavy metal detoxification and homeostasis. *Annual Review Plant Biology* **53,** 159–182.

Cobbett C.S., May M.J., Howden R. & Rolls B. (1998) The glutathione-deficient, cadmium-sensitive mutant, *cad2-1*, of *Arabidopsis thaliana* is deficient in γ-glutamylcysteine synthetase. *The Plant Journal* **16,** 73–78.

De la Rosa G., Peralta-Videa J.R., Montes M., Parsons J.G., Cano-Aguilera I. & Gardea-Torresdey J.L. (2004) Cadmium uptake and translocation in tumbleweed (*Salsola kali*), a potential Cd-hyperaccumulator desert plant species: ICP/OES and XAS studies. *Chemosphere* **55,** 1159–1168.

Gardea-Torresdey J.L., Gomez E., Peralta-Videa J.R., Tiemann K.J., Parsons J.G., Trolani H. & Yacaman M.J. (2003) Use of XAS and TEM to determine the uptake of gold and silver and nanoparticle formation by living alfalfa plants. *Proceedings of the 225th American Chemical Society National Meeting, Division of Environmental Chemistry* **43,** 1016–1022.

Göthberg A. & Greger M. (2006) Formation of methyl mercury in an aquatic macrophyte. *Chemosphere* **65,** 2096–2105.

Greger M. & Dabrowska B. (2010) Influence of nutrient level on methylmercury content in water spinach. *Environmental Toxicology and Chemistry* **29,** 1735–1739.

Grill E., Löffler S., Winnacker E.L. & Zenk M.H. (1989) Phytochelatins, the heavy-metal-binding peptides of plants, are synthesized from glutathione by a specific γ-glutamylcysteine dipeptidyl transpeptidase (phytochelatin synthase). *Proceedings of the National Academy of Sciences of the United States of America* **86,** 6838–6842.

Ha S.B., Smith A.P., Howden R., Dietrich W.M., Bugg S., O'Connell M.J., Goldsbrough P.B. & Cobbett C.S. (1999) Phytochelatin synthase genes from *Arabidopsis* and the yeast *Schizosaccharomyces pombe*. *The Plant Cell* **11,** 1153–1164.

Hall J.L. (2002) Cellular mechanisms for heavy metal detoxification and tolerance. *Journal Experimental Botany* **52,** 631–640.

Haydon M.J. & Cobbett C.S. (2007) Transporters of ligands for essential metal ions in plants. *New Phytologist* **174,** 499–506.

Howden R., Goldsbrough P.B., Andersen C.R. & Cobbett C.S. (1995) Cadmium-sensitive, *cad1* mutants of *Arabidopsis thaliana* are phytochelatin deficient. *Plant Physiology* **107,** 1059–1066.

Iglesia-Turiño S., Febrero A., Jauregui O., Caldelas C., Araus J.L. & Bort J. (2006) Detection and quantification of unbound phytochelatin 2 in plant extracts of *Brassica napus* grown with different levels of mercury. *Plant Physiology* **142,** 742–749.

Isaure M.P., Fayard B., Sarret G., Pairis S. & Bourguignon J. (2006) Localization and chemical forms of cadmium in plant samples combining analytical electron microscopy and X-ray spectromicroscopy. *Spectrochimica Acta Part B* **61,** 1242–1252.

Kim C.S., Brown G.E. & Rytuba J.J. (2000) Characterization and speciation of mercury-bearing mine waste using X-ray absorption spectroscopy. *Science of the Total Environment* **261,** 157–168.

Krupp E.M., Milne B.F., Mestrot A., Meharg A.A. & Feldmann J. (2008) Investigation into mercury bound to biothiols: structural identification using ESI-ion-trap MS and introduction of a method for their HPLC separation with simultaneous detection by ICP-MS and ESI-MS. *Annals of Bioanalytical Chemistry* **390,** 1753–1764.

Krupp E.M., Mestrot A., Wielgus J., Meharg A.A. & Feldmann J. (2009) The molecular form of mercury in biota: identification of novel mercury peptide complexes in plants. *Chemical Communications* **28,** 4257–4259.

Leonard T.L., Taylor G.E. Jr, Gustin M.S. & Fernandez G.C.J. (1998) Mercury and plants in contaminated soils: uptake, partitioning and emission to the atmosphere. *Environmental Toxicology Chemistry* **17,** 2063–2071.

Lombi E., Scheckel K.G., Pallon J., Carey A.M., Zhu Y.G. & Meharg A.A. (2009) Speciation and distribution of arsenic and localization of nutrients in rice grains. *New Phytologist* **184,** 193–201.

Lombi E. & Susini J. (2009) Synchrotron-based techniques for plant and soil science: opportunities, challenges and future perspectives. *Plant and Soil* **320,** 1–35.

Loscos J., Naya L., Ramos J., Clemente M.R., Matamoros M.A. & Becana M. (2006) A reassessment of substrate specificity and activation of phytochelatin synthases from model plants by physiologically relevant metals. *Plant Physiology* **140,** 1213–1221.

Lozano-Rodríguez E., Hernández L.E., Bonay P. & Carpena-Ruiz R.O. (1997) Distribution of cadmium in shoot and root tissues of maize and pea plants: physiological disturbances. *Journal of Experimental Botany* **48,** 123–128.

Mehra R.K., Miclat J., Kodati V.R., Abdullah R., Hunter T.C. & Mulchandani P. (1996) Optical spectroscopic and reverse-phase HPLC analyses of Hg(II) binding to phytochelatins. *Biochemical Journal* **314,** 73–82.

Meuwly P., Thibaul P., Schwan A.L. & Rauser W.E. (1995) Three families of thiol peptides are induced by cadmium in maize. *The Plant Journal* **7,** 391–400.

Nriagu J.O. (1990) Global metal pollution. *Environment* **32,** 7–33.

Ortega-Villasante C., Rellán-Álvarez R., del Campo F.F., Carpena-Ruiz R.O. & Hernández L.E. (2005) Cellular damage induced by cadmium and mercury in *Medicago sativa*. *Journal of Experimental Botany* **56,** 2239–2251.

Ortega-Villasante C., Hernández L.E., Rellán-Álvarez R., del Campo F.F. & Carpena-Ruiz R.O. (2007) Rapid alteration of cellular redox homeostasis upon exposure to cadmium and mercury in alfalfa seedlings. *New Phytologist* **176,** 96–107.

Patty C., Barnett B., Mooney B., Kahn A., Levy S., Liu Y.J., Pianetta P. & Andrews J.C. (2009) Using X-ray microscopy and Hg L-3 XANES to study Hg binding in the rhizosphere of *Spartina* cordgrass. *Environmental Science Technology* **43,** 7397–7402.

Pickering I.J., Wright C., Bubner B., Ellis D., Persans M.W., Yu E.Y., George G.N., Prince R.C. & Salt D.E. (2003) Chemical form and distribution of selenium and sulphur in the selenium hyperaccumulator *Astragalus bisulcatus*. *Plant Physiology* **131,** 1460–1467.

Punshon T., Guerinot M.L. & Lanzirotti A. (2009) Using synchrotron X-ray fluorescence microprobes in the study of metal homeostasis in plants. *Annals of Botany* **103,** 665–672.

Rajan M., Darrow J., Hua M., Barnett B., Mendoza M., Greenfield B.K. & Andrews J.C. (2008) Hg L3 XANES study of mercury methylation in shredded *Eichhornia crassipes*. *Environmental Science Technology* **42,** 5568–5573.

Rauser W.E. & Meuwly P. (1995) Retention of cadmium in roots of maize seedlings. *Plant Physiology* **109,** 195–202.

Rellán-Álvarez R., Ortega-Villasante C., Álvarez-Fernández A., del Campo F.F. & Hernández L.E. (2006a) Stress responses of *Zea mays* to cadmium and mercury. *Plant and Soil* **279,** 41–50.

Rellán-Álvarez R., Hernández L.E., Abadía J. & Álvarez-Fernández A. (2006b) Direct and simultaneous determination of reduced and oxidized glutathione and homoglutathione by liquid chromatography electrospray/mass spectrometry in plant tissue extracts. *Analytical Biochemistry* **356,** 254–264.

Riddle S.G., Tran H.H., Dewitt J.G. & Andrews J.C. (2002) Field, laboratory, and X-ray absorption spectroscopic studies of mercury accumulation by water hyacinths. *Environmental Science Technology* **36,** 1965–1970.

Salt D.E., Prince R.C. & Pickering I.J. (2002) Chemical speciation of accumulated metals in plants: evidence from X-ray absorption spectroscopy. *Microchemical Journal* **71,** 255–259.
Schützendübel A. & Polle A. (2002) Plant responses to abiotic stresses: heavy metal-induced oxidative stress and protection by mycorrhization. *Journal of Experimental Botany* **53,** 1351–1365.
Sharma S.S. & Dietz K.J. (2006) The significance of amino acids and amino acid-derived molecules in plant responses and adaptation to heavy metal stress. *Journal of Experimental Botany* **57,** 711–726.
Sobrino-Plata J., Ortega-Villasante C., Flores-Cáceres M.L., Escobar C., Del Campo F.F. & Hernández L.E. (2009) Differential alterations of antioxidant defenses as bioindicators of mercury and cadmium toxicity in alfalfa. *Chemosphere* **77,** 946–954.
Suszcynsky E.M. & Shann J.R. (1995) Phytotoxicity and accumulation of mercury in tobacco subjected to different exposure routes. *Environmental Toxicology Chemistry* **14,** 61–67.
Válega M., Lima A.I.G., Figueira E.M.A.P., Pereira E., Pardal M.A. & Duarte A.C. (2009) Mercury intracellular partitioning and chelation in a salt marsh plant, *Halimione portulacoides* (L.) Aellen: strategies underlying tolerance in environmental exposure. *Chemosphere* **74,** 530–536.
Van Assche F. & Clijsters H. (1990) Effects of metals on enzyme activity in plants. *Plant, Cell & Environment* **13,** 195–206.
Vatamaniuk O.K., Mari S., Lu Y.P. & Rea P.A. (1999) AtPCS1, a phytochelatin synthase from Arabidopsis: isolation and *in vitro* reconstitution. *Proceedings of the National Academy of Sciences of the United States of America* **96,** 7110–7115.
Vatamaniuk O.K., Mari S., Lu Y.P. & Rea P.A. (2000) Mechanism of heavy metal ion activation of phytochelatin (PC) synthase – blocked thiols are sufficient for PC synthase-catalyzed transpeptidation of glutathione and related thiol peptides. *Journal of Biological Chemistry* **275,** 31451–31459.
Vatamaniuk O.K., Mari S., Lang A., Chalasani S., Demkiv L.O. & Rea P. (2004) Phytochelatin synthase, a dipeptidyl transferase that undergoes multisite acylation with gammaglutamylcysteine during catalysis. Stoichiometric and site-directed mutagenic analysis of AtPCS1-catalyzed phytochelatin synthesis. *Journal of Biological Chemistry* **279,** 22449–22460.
Webb S.M. (2005) Sixpack: a graphical user interface for XAS analysis using IFEEF IT. *Physica Scripta* **115,** 1011–1014.
Zhang Z.C., Chen B.X. & Qiu B.S. (2010) Phytochelatin synthesis plays a similar role in shoots of the cadmium hyperaccumulator *Sedum alfredii* as in non-resistant plants. *Plant, Cell & Environment* **33,** 1248–1255.

Received 8 September 2010; received in revised form 4 December 2010; accepted for publication 21 December 2010

SUPPORTING INFORMATION

Additional Supporting Information may be found in the online version of this article:

Figure S1. Experimental and theoretical isotopic signatures of the identified Hg-containing ions found in the HPLC-ESI/TOFMS analysis of the root soluble fraction from 3-week-old alfalfa (A-R), barley (S-U) and maize (V-Z) plants treated with 30 μM $HgCl_2$ for 7 d.
Figure S2. Correlation diagram of S relative to Hg, obtained from Fig. 2 as fluorescence line intensity (counts s^{-1}), in roots of alfalfa plants treated with 30 μM for 7 d, after analysis by μ-SXRF.
Figure S3. Biothiol profile of *Arabidopsis thaliana* Col-0, *cad2-1* and *cad1-3* leaves infiltrated with control (0), 30 μM Cd or 30 μM Hg for 48 h. Peaks were identified by the elution of commercially available standards. Concentration was calculated by the integration of the internal standard N-acetyl-cysteine (Peak 3): Cys (1), GSH (2), PC_2 (4). PC_3 (5), PC_4 (6), and PC_5 (7).
Figure S4. Assay to identify Hg-GSH complexes with respect to the detection limit of the HPLC-ESI-TOFMS analysis. Theoretical (**A**) isotopic signature of $[Hg(GSH)_2–H]^-$ ion at m/z 813.1 found detected in *A. thaliana* Col-0 leaves infiltrated with 30 μM Hg for 48 h and spiked with 25 μM Hg:50 μM GSH (**B**), 2.5 μM Hg:5 μM GSH (**C**), and with deionized water (**D**).
Table S1. Species observed, mass charge ratio (m/z) and retention time for LC – ESI/MS(TOF) analysis with positive and negative ionization modes of biothiols and Hg biothiols complexes standard solutions. The ratio Hg:ligand was (μM) 10:10; 10:20; 20:10. Identity of each complex was confirmed by the simulation of theoretical spectra with the MicrOtof Data Analysis Software. Ions are ordered by increasing m/z value.

Please note: Wiley-Blackwell are not responsible for the content or functionality of any supporting materials supplied by the authors. Any queries (other than missing material) should be directed to the corresponding author for the article.